blood®
Regular Article

MYELOID NEOPLASIA

CME Article

SETD2 deficiency accelerates MDS-associated leukemogenesis via S100a9 in *NHD13* mice and predicts poor prognosis in MDS

Bing-Yi Chen,[1,2,*] Junhong Song,[3,*] Cheng-Long Hu,[1,*] Shu-Bei Chen,[2,4] Qunling Zhang,[5] Chun-Hui Xu,[1] Ji-Chuan Wu,[1] Dan Hou,[1] Ming Sun,[1] Yuan-Liang Zhang,[2] Na Liu,[2] Peng-Cheng Yu,[1] Ping Liu,[1] Li-Juan Zong,[1] Jia-Ying Zhang,[1] Ruo-Fei Dai,[6] Fei Lan,[6] Qiu-Hua Huang,[2] Su-Jiang Zhang,[2] Stephen D. Nimer,[7] Zhu Chen,[2] Sai-Juan Chen,[2] Xiao-Jian Sun,[2] and Lan Wang[1]

[1]CAS Key Laboratory of Tissue Microenvironment and Tumor, Shanghai Institute of Nutrition and Health, Shanghai Institutes for Biological Sciences, University of Chinese Academy of Sciences, Chinese Academy of Sciences, Shanghai, China; [2]State Key Laboratory of Medical Genomics, Shanghai Institute of Hematology, National Research Center for Translational Medicine, Ruijin Hospital, Shanghai Jiao Tong University School of Medicine, Shanghai, China; [3]Key Laboratory of Pediatric Hematology and Oncology, Ministry of Health, Department of Pediatric Hematology and Oncology, Shanghai Children's Medical Center, Shanghai Jiao Tong University School of Medicine, Shanghai, China; [4]Shanghai Jiao Tong University School of Life Sciences and Biotechnology, Shanghai, China; [5]Department of Medical Oncology, Fudan University Shanghai Cancer Center, Shanghai Medical College, Fudan University, Shanghai, China; [6]Liver Cancer Institute, Zhongshan Hospital, Fudan University, Key Laboratory of Carcinogenesis and Cancer Invasion, Ministry of Education and Institutes of Biomedical Sciences, Fudan University, Shanghai, China; and [7]Department of Medicine, University of Miami Miller School of Medicine, Miami, FL

KEY POINTS

- **Low expression of *SETD2* predicts poor prognosis in MDS, and loss of *Setd2* accelerates MDS-associated leukemogenesis in *NHD13* mice.**
- ***Setd2* deficiency impairs S100a9-mediated self-renewal and differentiation of HSPCs in *NHD13* mice.**

SETD2, the histone H3 lysine 36 methyltransferase, previously identified by us, plays an important role in the pathogenesis of hematologic malignancies, but its role in myelodysplastic syndromes (MDSs) has been unclear. In this study, low expression of *SETD2* correlated with shortened survival in patients with MDS, and the *SETD2* levels in CD34$^+$ bone marrow cells of those patients were increased by decitabine. We knocked out *Setd2* in *NUP98-HOXD13* (*NHD13*) transgenic mice, which phenocopies human MDS, and found that loss of *Setd2* accelerated the transformation of MDS into acute myeloid leukemia (AML). Loss of *Setd2* enhanced the ability of *NHD13*$^+$ hematopoietic stem and progenitor cells (HSPCs) to self-renew, with increased symmetric self-renewal division and decreased differentiation and cell death. The growth of MDS-associated leukemia cells was inhibited though increasing the H3K36me3 level by using epigenetic modifying drugs. Furthermore, *Setd2* deficiency upregulated hematopoietic stem cell signaling and downregulated myeloid differentiation pathways in the *NHD13*$^+$ HSPCs. Our RNA-seq and chromatin immunoprecipitation–seq analysis indicated that *S100a9*, the S100 calcium-binding protein, is a target gene of *Setd2* and that the addition of recombinant S100a9 weakens the effect of *Setd2* deficiency in the *NHD13*$^+$ HSPCs. In contrast, downregulation of *S100a9* leads to decreases of its downstream targets, including *Ikba* and *Jnk*, which influence the self-renewal and differentiation of HSPCs. Therefore, our results demonstrated that *SETD2* deficiency predicts poor prognosis in MDS and promotes the transformation of MDS into AML, which provides a potential therapeutic target for MDS-associated acute leukemia. (*Blood*. 2020;135(25):2271-2285)

All other clinicians completing this activity will be issued a certificate of participation. To participate in this journal CME activity: (1) review the learning objectives and author disclosures; (2) study the education content; (3) take the post-test with a 75% minimum passing score and complete the evaluation at **http://www.medscape.org/journal/blood**; and (4) view/print certificate. For CME questions, see page 2326.

Disclosures

Associate Editor Margaret A. Goodell, CME questions author Laurie Barclay, freelance writer and reviewer, Medscape, LLC, and the authors declare no relevant financial relationships.

Learning objectives

Upon completion of this activity, participants will be able to:

1. Describe the role of *SETD2* in the progression of myelodysplastic syndrome (MDS) to acute myeloid leukemia (AML), according to study results of *SETD2* expression in patients with MDS and of the effects of decitabine on *SETD2* levels in cluster of differentiation 34 (CD34)–positive bone marrow cells of patients with MDS
2. Determine the role of *SETD2* in the progression of MDS to AML, according to the effect of knockout of *Setd2* in the *NUP98-HOXD13* (*NHD13*) transgenic mouse model, which phenocopies human MDS
3. Identify clinical and research implications of the role of *Setd2* in the progression of MDS to AML, according to human and knockout mice studies

Release date: June 18, 2020; Expiration date: June 18, 2021

Introduction

Myelodysplastic syndrome (MDS) is one of the most common myeloid malignancies characterized by bone marrow (BM) dysplasia, inefficient hematopoiesis, cytopenia, and a risk of progression to acute myeloid leukemia (AML).[1,2] Several mouse models have been developed to mimic human MDS, and the *NUP98-HOXD13* (*NHD13*) transgenic mouse is probably the most accurate, in which *NHD13* is driven by the *Vav1* promoter to express in hematopoietic cells.[3] The *NHD13* mice show anemia, neutropenia, and lymphopenia with hypercellular/normocellular BM, suggesting ineffective hematopoiesis. It is also an excellent model for the study of MDS progression to leukemia, as approximately one-third of *NHD13* mice with MDS develop leukemia, most commonly AML, which mimics disease progression in MDS patients.[3,4] Mutations in epigenetic modifiers, such as *DNMT3A*, *TET2*, *EZH2*, *ASXL1*, and *BCOR*, are commonly found in, and contribute to, MDS.[5-9] Thus, MDS appears to be an epigenetic malignancy, consistent with its response to DNA demethylating drugs.[10-12] For example, decitabine, the hypomethylating agent, has been the standard of MDS treatment for more than a decade.[13]

We had identified the histone methyltransferase SETD2 as the only enzyme that catalyzes histone H3 lysine 36 trimethylation (H3K36me3) in mammals.[14,15] SETD2 binds to elongating RNA polymerase II and generates H3K36-trimethylated nucleosomes in the gene body regions of active genes, which provides docking sites for many important chromatin regulators, including DNMT3A/B.[14,16] We have studied the role of Setd2 in embryonic development and normal hematopoiesis using genetically modified mouse models. We reported that *Setd2* constitutive knockout mice exhibit embryonic lethality related to defects in embryonic vasculargenesis,[15] and we and others also established that hematopoiesis-specific *Setd2* deficiency impairs self-renewal and differentiation of hematopoietic stem cells (HSCs).[17,18]

SETD2 has been found to be mutated in different types of acute leukemia, including ~6% of AML cases and ~10% of cases of acute lymphoid leukemia.[19-21] A particularly high frequency (22%) of *SETD2* mutation is associated with *MLL*-rearranged leukemia.[20] *SETD2* genetic polymorphisms are also associated with AML prognosis.[22] In the *MLL*-fusion–driven mouse BM transplantation models of AML, loss of a single allele of *Setd2* or knockdown of *Setd2* increases the growth of AML cells and shortens disease latency.[20,23,24] However, it has also been observed that a complete loss of *Setd2* (eg, by deletion of both alleles of *Setd2*) blocks development of leukemia.[23-25] These studies indicate a pivotal but complicated role of Setd2 in the pathogenesis of acute leukemia.

Some studies have shown that *NHD13*-induced MDS/leukemia is controlled by epigenetic regulators (eg, MLL1, NSL, and p300), transcription factors (eg, p53 and Lmo2/Lyl1), HSC regulators (eg, MSI2 and Flt3), and apoptosis-related proteins (eg, Bcl2, PKR, and Puma). However, the role of SETD2 in the pathogenesis of *NHD13* MDS/AML is unknown. Consistent with the above-described evidence implicating Setd2 as a tumor suppressor, we recently found that the *Mx1*-Cre–driven *Setd2*-knockout mice develop MDS when aged, indicating the causal function of SETD2 in myeloid malignancies.[17] Both nonsense and frameshift-deletion mutations of *SETD2* have been identified in MDS patients.[26] Our clinical analysis showed that low expression of *SETD2* was associated with shorter survival in MDS patients, and thus we hypothesized that SETD2 plays a vital role in the progression of MDS to AML.

Materials and methods

MDS patients

The microarray data, which contains data of 183 MDS patients and 17 control samples, are available at GEO (GSE19429).[27] The cDNA, BM paraffin-embedded sections, and BM cells of MDS patients and samples from healthy subjects were collected from Shanghai Children's Medical Center by J.S.

Mice

The *NHD13* transgenic mice were purchased from Jackson Laboratory, and the *Setd2*$^{flox/flox}$ (*Setd2*$^{f/f}$) mice were bred as described previously.[17] The *Mx1-Cre* mice and CD45.1 B6SJL mice were purchased from Shanghai Research Center for Model Organisms.

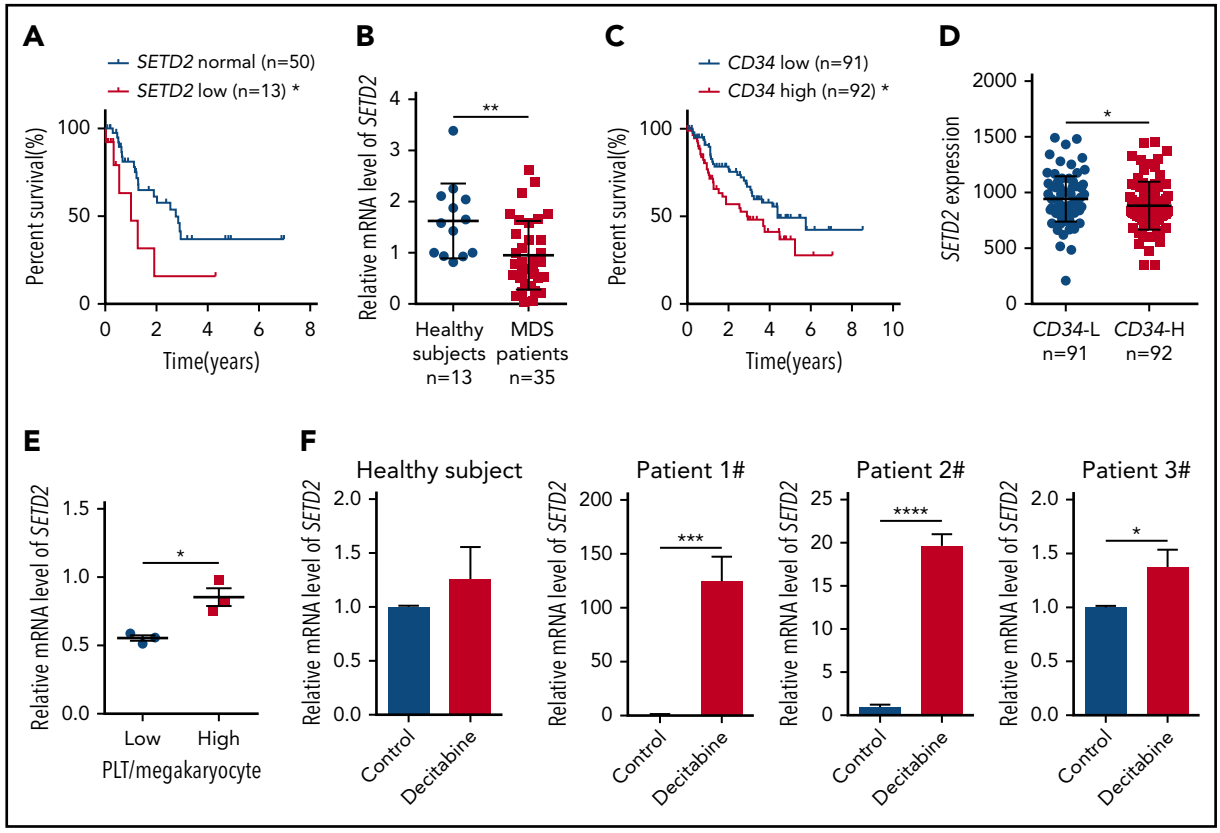

Figure 1. Low expression of *SETD2* predicts a poor outcome in MDS patients. (A) Overall survival of patients with refractory anemia with excess blasts, a subtype of MDS, was stratified by *SETD2* expression into *SETD2* low (z score < -0.9; n = 13; median survival, 1.0 year) and normal ($-0.9 \leq$ z score ≤ 0.9; n = 50; median survival, 2.8 years) groups. Statistical significance was evaluated by log-rank test. (B) qPCR analysis of expression of *SETD2* in BM mononuclear cells from healthy subjects (n = 13) and MDS patients (n = 35). (C) Overall survival of the MDS patients stratified by *CD34* expression. The absolute average of relative *CD34* expression was used as the criterion to stratify the patients into *CD34* low (n = 91; median survival, 4.4 years) and high (n = 92; median survival, 2.9 years) groups. (D) Differential expression of *SETD2* in the $CD34^+$ cells of MDS patients with *CD34* low (L) and high (H) expression. The same criterion was used to stratify the patients as in panel C. (E) qPCR analysis of *SETD2* expression in the BM $CD34^+$ cells of the MDS patients with low or high platelet (PLT)/megakaryocyte counts. (F) qPCR analysis of *SETD2* expression in the primary BM $CD34^+$ cells treated with 5 nM decitabine or vehicle control for 48 hours. The patient samples in panels A, C, and D are from GEO (GSE19429) expression microarrays, and those in the other panels are from our own samples. $^*P < .05$; $^{**}P < .01$; $^{***}P < .001$; $^{****}P < .0001$.

The *NHD13* mice were crossed with *Mx1*-Cre/*Setd2*$^{f/f}$ or *Setd2*$^{f/f}$ mice, and *Setd2* was deleted by injection of poly(I:C) into *Mx1*-Cre/*NHD13*/*Setd2*$^{f/f}$ mice, relative to control *NHD13*/*Setd2*$^{f/f}$ mice. All mice used in the experiments were on a pure C57BL/6 genetic background. The mice were used according to animal care standards, and animal studies were approved by the Committee of Animal Use at Shanghai Institute of Nutrition and Health.

Results

Low expression of *SETD2* predicts poor prognosis in MDS

To investigate the role of *SETD2* in MDS, we first used microarray-based gene expression profiling data of primary BM $CD34^+$ cells from 183 MDS patients[27] to learn whether the expression of *SETD2* is associated with prognosis. The results showed that, in refractory anemia with excess blasts, a high-risk subtype of MDS, patients with low *SETD2* expression had a significantly worse overall survival than the patients with normal *SETD2* expression (Figure 1A), whereas the high-*SETD2* group showed no significant difference (supplemental Figure 1A; available on the *Blood* Web site). We then performed quantitative polymerase chain reaction (qPCR) analysis of our MDS patient samples, and the results showed that the expression of *SETD2* was significantly lower in the MDS patient samples than in those from healthy subjects (Figure 1B). Given the association of high *CD34* expression with short survival in MDS patients (Figure 1C), we further analyzed the microarray data of the MDS patient samples, and we found that the expression of *SETD2* correlated negatively with *CD34* expression (Figure 1D). SETD2 is the only enzyme responsible for H3K36me3, and we therefore performed immunohistochemical analysis of MDS patient BM samples, using anti-H3K36me3 or CD34 antibodies. The results showed that H3K36me3 correlated negatively with CD34 expression (supplemental Figure 1B-C), consistent with the microarray analysis. In addition, the MDS patients with a low platelet/megakaryocyte ratio showed less *SETD2* expression than those with a higher platelet/megakaryocyte ratio (Figure 1E). We did not observe a correlation of low expression of *SETD2* with known MDS-associated gene mutations such as *NF1*, *PTPN11*, *KRAS*, *NRAS*, *RUNX1*, or *SH2B3*, in the analyzed MDS patient samples (supplemental Figure 1D). Low expression of *SETD2* is associated with short survival in MDS, and we hypothesized that *SETD2* expression could be altered by therapeutic drug treatments. To test this hypothesis, we used decitabine, a demethylating agent commonly used in MDS therapy, to treat BM $CD34^+$ cells from MDS patients. qPCR analysis showed that *SETD2* expression was upregulated

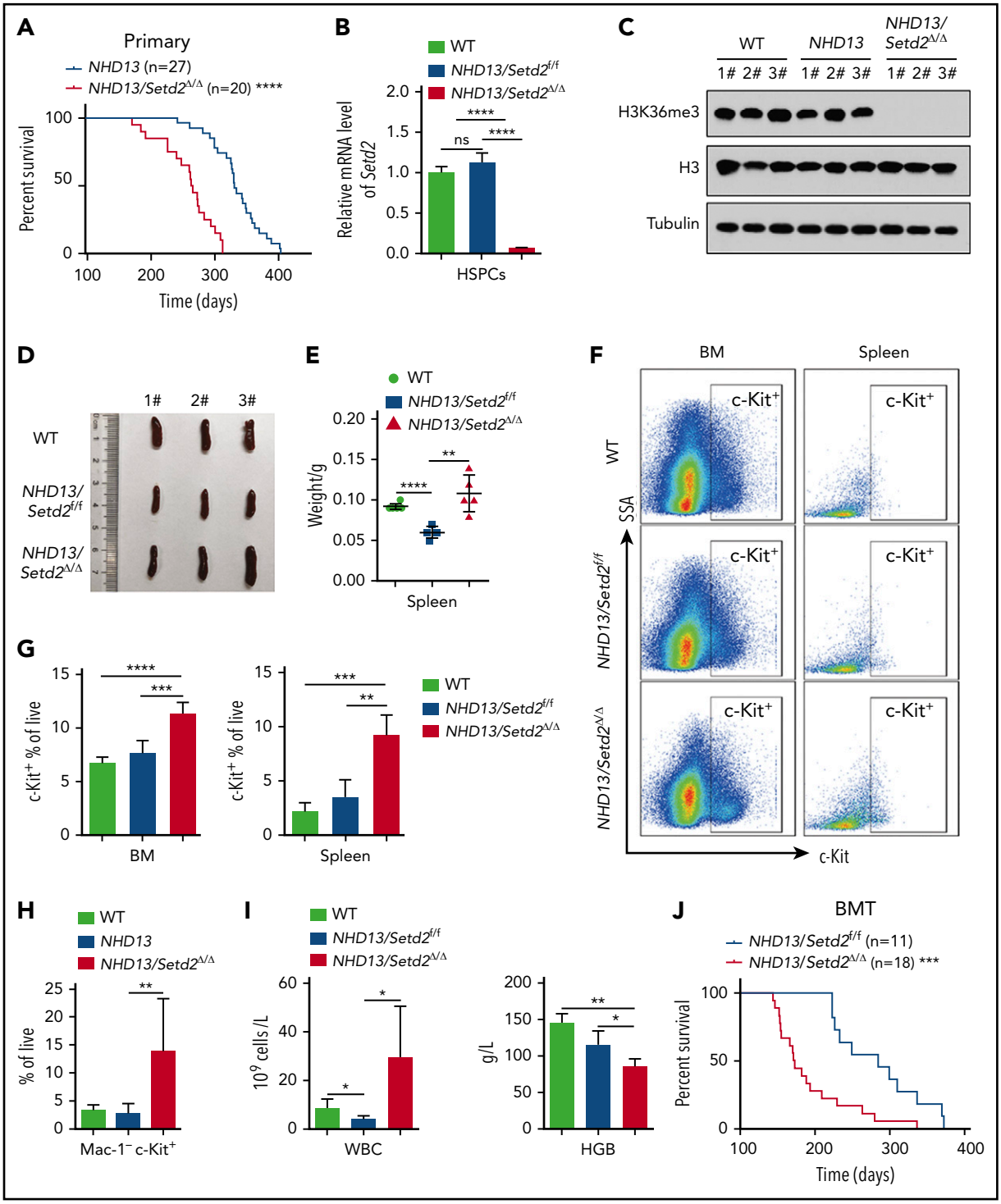

Figure 2. Deletion of *Setd2* accelerates the transformation of MDS to AML in the *NHD13* mouse model. (A) Survival curves of *NHD13* (n = 27; median survival, 333 days) and *NHD13/Setd2*$^{\Delta/\Delta}$ (n = 20; median survival, 267 days) mice. Poly(I:C) was injected into 6- to 8-week-old *Mx1*-Cre/*NHD13/Setd2*$^{f/f}$ mice. (B) qPCR analysis of *Setd2* expression in the BM HSPCs of the WT, *NHD13*, and *NHD13/Setd2*$^{\Delta/\Delta}$ mice. (C) Western blot analysis showing the abolishment of H3K36me3, which reflected the knockout efficiency of *Setd2*, in the BM cells isolated from the *NHD13/Setd2*$^{\Delta/\Delta}$ mice compared with the *NHD13* and WT mice. (D-E) Different size and weight of the spleens of the *NHD13/Setd2*$^{\Delta/\Delta}$, *NHD13*, and WT mice (n = 5). (F-G) Representative flow cytometry profiles (F) and quantification of the frequencies (G) of the c-Kit$^+$ cells in the BM and spleen of the indicated mice at 4 weeks after poly(I:C) injection. (H) Frequencies of the Mac-1$^-$c-Kit$^+$ cells in the BM of the *NHD13/Setd2*$^{\Delta/\Delta}$ mice during the leukemia stage, compared with the *NHD13* and WT mice. (I) Complete blood count (CBC) analysis of the WT, *NHD13*, and *NHD13/Setd2*$^{\Delta/\Delta}$ mice at 6 months after poly(I:C) injection. (J) Survival curves of the mice receiving *NHD13/Setd2*$^{f/f}$ (n = 11; median survival, 284 days) and *Mx1*-Cre/*NHD13/Setd2*$^{f/f}$ (n = 18; median survival, 172 days) BM cells. The mice were injected with poly(I:C) at 4 weeks after transplantation. *$P < .05$; **$P < .01$; ***$P < .001$; ****$P < .0001$.

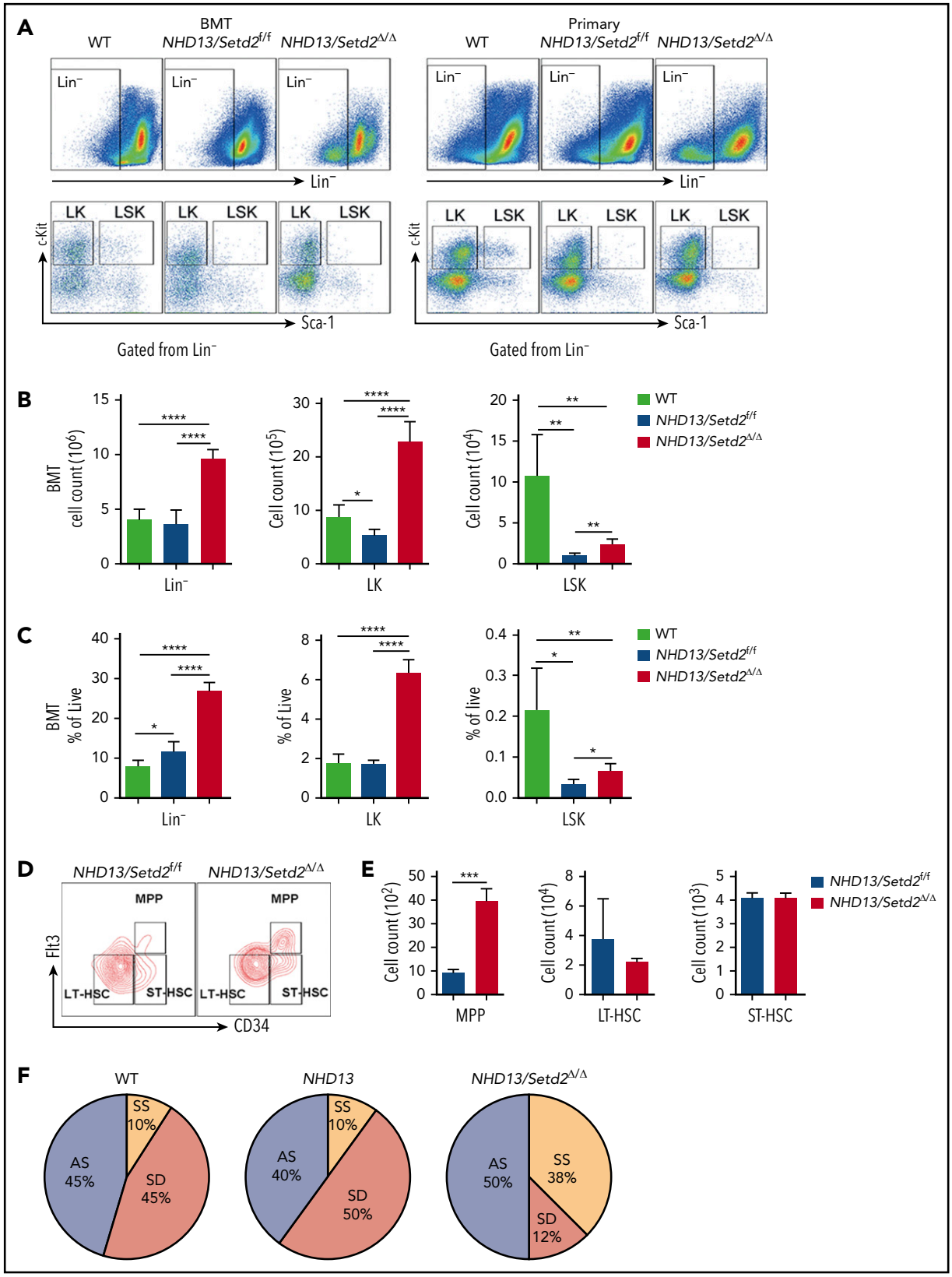

Figure 3. Loss of *Setd2* promotes self-renewal of HSCs in the *NHD13* mouse model. (A) Representative flow cytometry profiles of the Lin$^-$, LK, and LSK cells in the BM of the transplant-recipient mice (left) and the primary BM cells (right) of the *NHD13/Setd2*$^{f/f}$ or Mx1-Cre/*NHD13/Setd2*$^{f/f}$ mice at 4 weeks after poly(I:C) injection. (B-C) Quantification of the numbers (B) and frequencies (C) of the Lin$^-$, LK, and LSK cells in the BM of the transplant-recipient mice. (D-E) Representative flow cytometry profiles (D) and quantification of the frequencies (E) of the MPPs, LT-HSCs, and ST-HSCs of the *NHD13/Setd2*$^{f/f}$ and *NHD13/Setd2*$^{\Delta/\Delta}$ mice at 4 weeks after poly(I:C) injection. (F) The paired daughter cell assay analysis of the LSK cells isolated from BM of the *NHD13/Setd2*$^{f/f}$ or *NHD13/Setd2*$^{\Delta/\Delta}$ mice at 4 weeks after poly(I:C) injection. *$P < .05$; **$P < .01$; ***$P < .001$; ****$P < .0001$. AS, asymmetric self-renewal division; SD, symmetric commitment division; SS, symmetric self-renewal division.

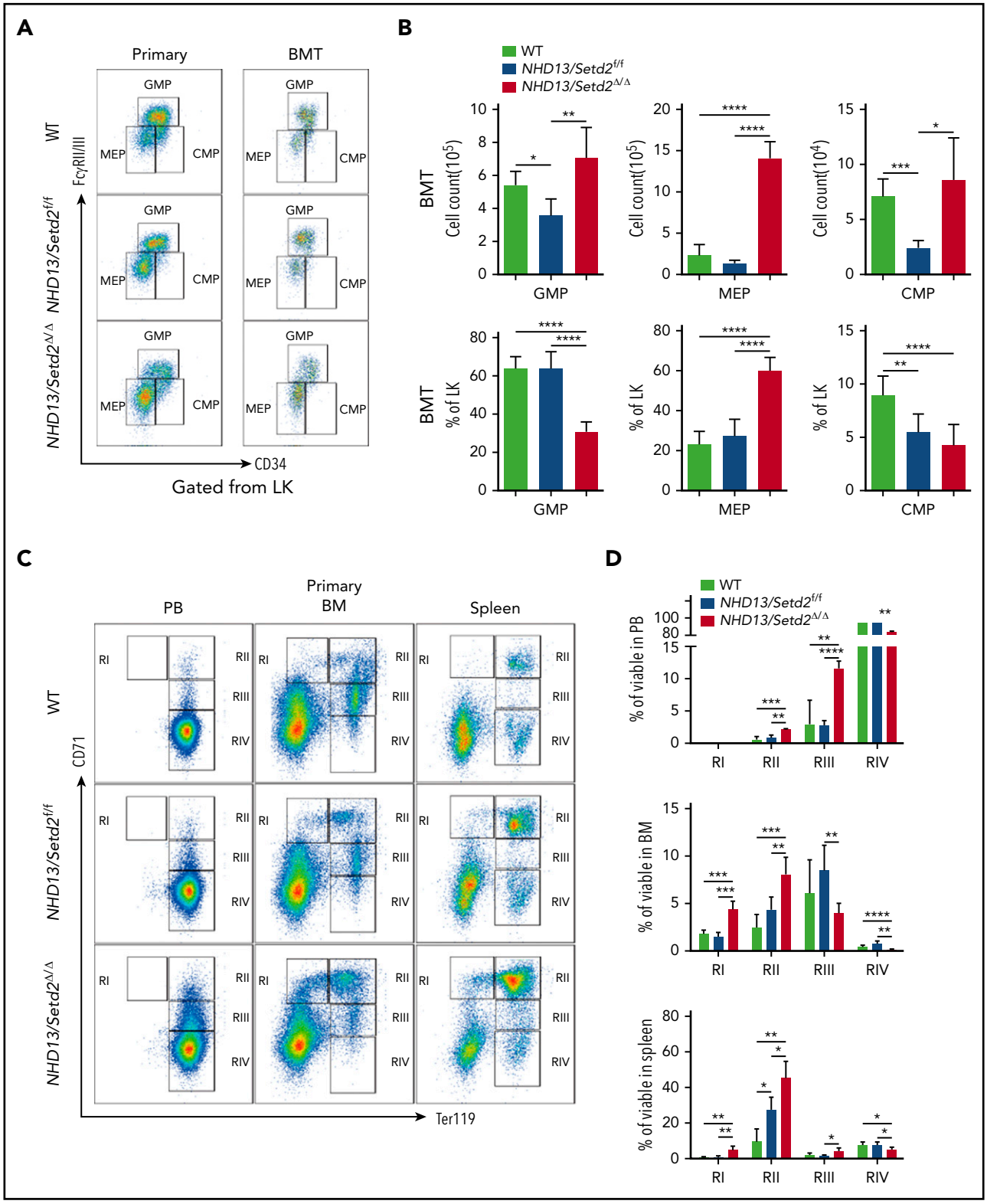

Figure 4. Deletion of *Setd2* affects the myeloid differentiation and cell cycle in the *NHD13* mouse model. (A-B) Representative flow cytometry profiles (A) and quantification of the cells counts and frequencies (B) of the GMP, MEP, and CMP cells of the mice receiving *NHD13/Setd2*$^{f/f}$ or Mx1-Cre/*NHD13/Setd2*$^{f/f}$ BM cells. (C-D) Representative flow cytometry profiles (C) and quantification of the frequencies (D) of the PB, BM, and spleen cells of the WT, *NHD13/Setd2*$^{f/f}$, and *NHD13/Setd2*$^{\Delta/\Delta}$ mice at the indicated erythroid differentiation stages (RI, proerythroblasts; RII, basophilic erythroblasts; RII, chromatophilic erythroblasts; RIV, orthochromatophilic erythroblasts). (E) CFU assays analyzing the HSPCs isolated from the mice receiving *NHD13/Setd2*$^{f/f}$ or Mx1-Cre/*NHD13/Setd2*$^{f/f}$ BM cells. The representative images of CFUs are shown. Cells (3×10^3) were plated for each assay. (F) Quantification of the number of colonies of burst-forming unit-erythroid (BFU-E), colony-forming unit-granulocyte (CFU-G), colony-forming unit-macrophage (CFU-M), and colony-forming unit-granulocyte, macrophage (CFU-GM) cells. (G) Representative flow cytometry results of the BrdU incorporation assay and (H) quantification of the frequencies of the BM Lin$^-$ cells of the *NHD13/Setd2*$^{f/f}$ or *NHD13/Setd2*$^{\Delta/\Delta}$ mice at the indicated cell cycle stages. The cells were collected at 4 weeks after poly(I:C) injection. *$P < .05$; **$P < .01$; ***$P < .001$; ****$P < .0001$.

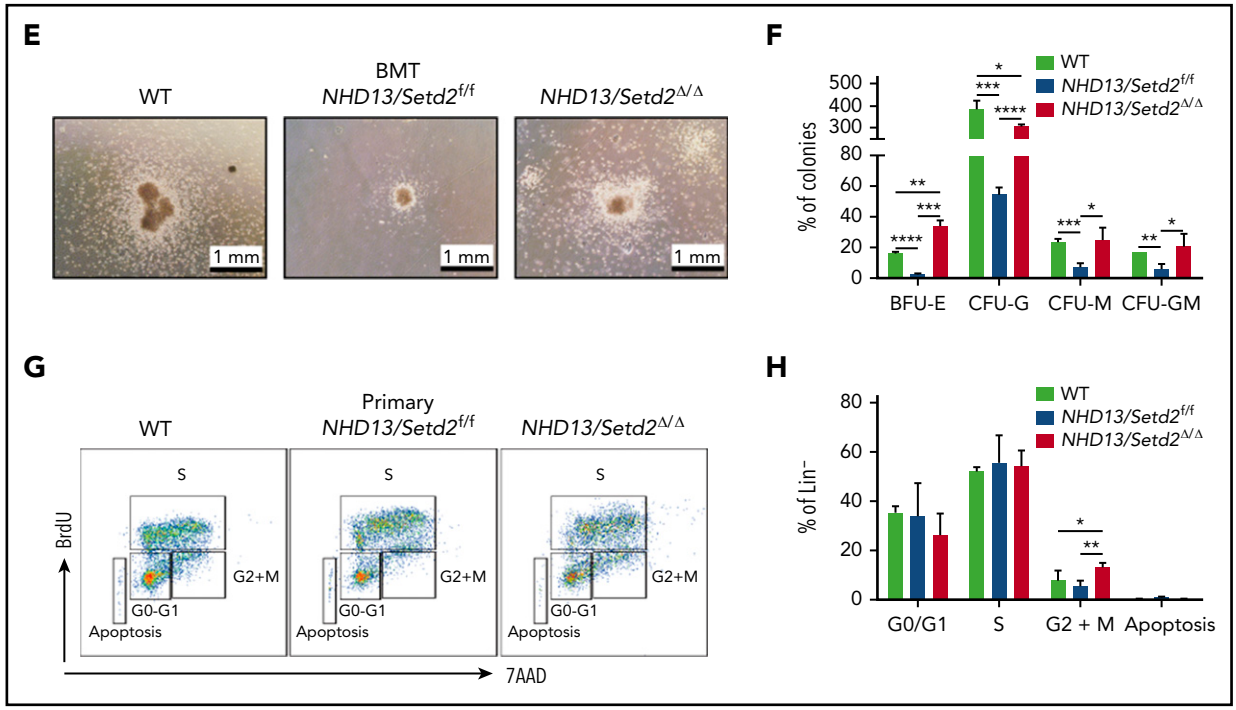

Figure 4. (Continued).

significantly by decitabine, albeit with variable fold change, in the MDS samples, but not in the samples from healthy subjects (Figure 1F). The variable fold change was not related to the basic level of *SETD2* expression (supplemental Figure 1E). As expected, decitabine significantly reduced the number of colonies produced by the primary MDS cells in the colony-forming unit (CFU) assay (supplemental Figure 1F-G). Thus, the increased expression of *SETD2* may indicate a good response to decitabine treatment in MDS patients. Altogether, our clinical sample analysis suggests that low expression of *SETD2* indicates a poor prognosis in MDS patients.

Setd2 deficiency accelerates the transformation of MDS to AML in the *NHD13* mice

To examine whether *Setd2* is crucial for MDS progression to AML, we crossed *NHD13* mice with *Setd2* conditional knockout mice (supplemental Figure 2A-B). The *NHD13/Setd2*$^{\Delta/\Delta}$ mice developed AML with a shorter median survival (267 days) than that of the *NHD13* mice (333 days; $P < .0001$; Figure 2A; supplemental Table 1). The expression of *Setd2* decreased significantly in the *NHD13/Setd2*$^{\Delta/\Delta}$ BM cells (Figure 2B), and H3K36me3 was abolished by *Setd2* deletion (Figure 2C), whereas the H3K36me2 level was not changed (supplemental Figure 2C). The spleens of the *NHD13/Setd2*$^{\Delta/\Delta}$ mice were enlarged compared with those of the *NHD13* and wild-type (WT) mice (Figure 2D-E). Phenotypically, all the *NHD13/Setd2*$^{\Delta/\Delta}$ mice had an increased percentage of c-Kit$^+$ cells in the BM and spleen compared with the *NHD13* mice (Figure 2F-G). At the leukemia stage, the percentage of Mac-1$^-$c-Kit$^+$ cells in the *NHD13/Setd2*$^{\Delta/\Delta}$ mice was higher than in the *NHD13* mice (Figure 2H), which was consistent with our morphology analysis results showing that the *NHD13/Setd2*$^{\Delta/\Delta}$ AML cells had less myeloid differentiation (supplemental Figure 2D). The leukemic *NHD13/Setd2*$^{\Delta/\Delta}$ mice had enlarged spleens and livers (supplemental Figure 2E) and extensive extramedullary hematopoiesis and infiltration of myeloblasts in multiple organs (supplemental Figure 2F), as well as increased white blood cell (WBC) counts and decreased hemoglobin (HGB) levels compared with age-matched *NHD13* mice (Figure 2I). Notably, analyses of the mice at relatively early, nonleukemic stages showed that the deletion of *Setd2* could modify the *NHD13*-driven phenotypes in a short period (supplemental Figure 2G-H), indicating a direct rather than secondary effect. In addition, single-allele deletion of Setd2 could not accelerate leukemia progression in the *NHD13* mice (supplemental Figure 3A), although it caused spleen and liver enlargement (supplemental Figure 3B) and a relatively high number of myeloblasts (supplemental Figure 3C-D). These observations imply that *Setd2* plays a unique role in *NHD13*–associated, relative to *MLL*-fusion–associated, leukemia models.

To further study the effect of *Setd2* on MDS-associated leukemia, *NHD13* and *NHD13/Setd2*$^{\Delta/\Delta}$ BM cells were transplanted into lethally irradiated recipient mice, and *Setd2* was deleted in the recipient mice at 4 weeks after transplantation by poly(I:C) injection (supplemental Figure 4A-B). Consistent with the observations in the primary mice, *Setd2* deficiency accelerated the development of AML and shortened survival in the transplant-recipient mice, as well (Figure 2J). Whereas the *NHD13* mice died of MDS/leukemia, with a median survival of 284 days, all the *NHD13/Setd2*$^{\Delta/\Delta}$ recipient mice died of AML, with a median survival of 172 days (Figure 2J). The leukemic mice receiving transplants of *NHD13/Setd2*$^{\Delta/\Delta}$ BM cells had significantly enlarged spleens (supplemental Figure 4C) and had more leukemia blast cells in spleen and liver in the histology analysis (supplemental Figure 4D) than did the *NHD13*-recipient mice.

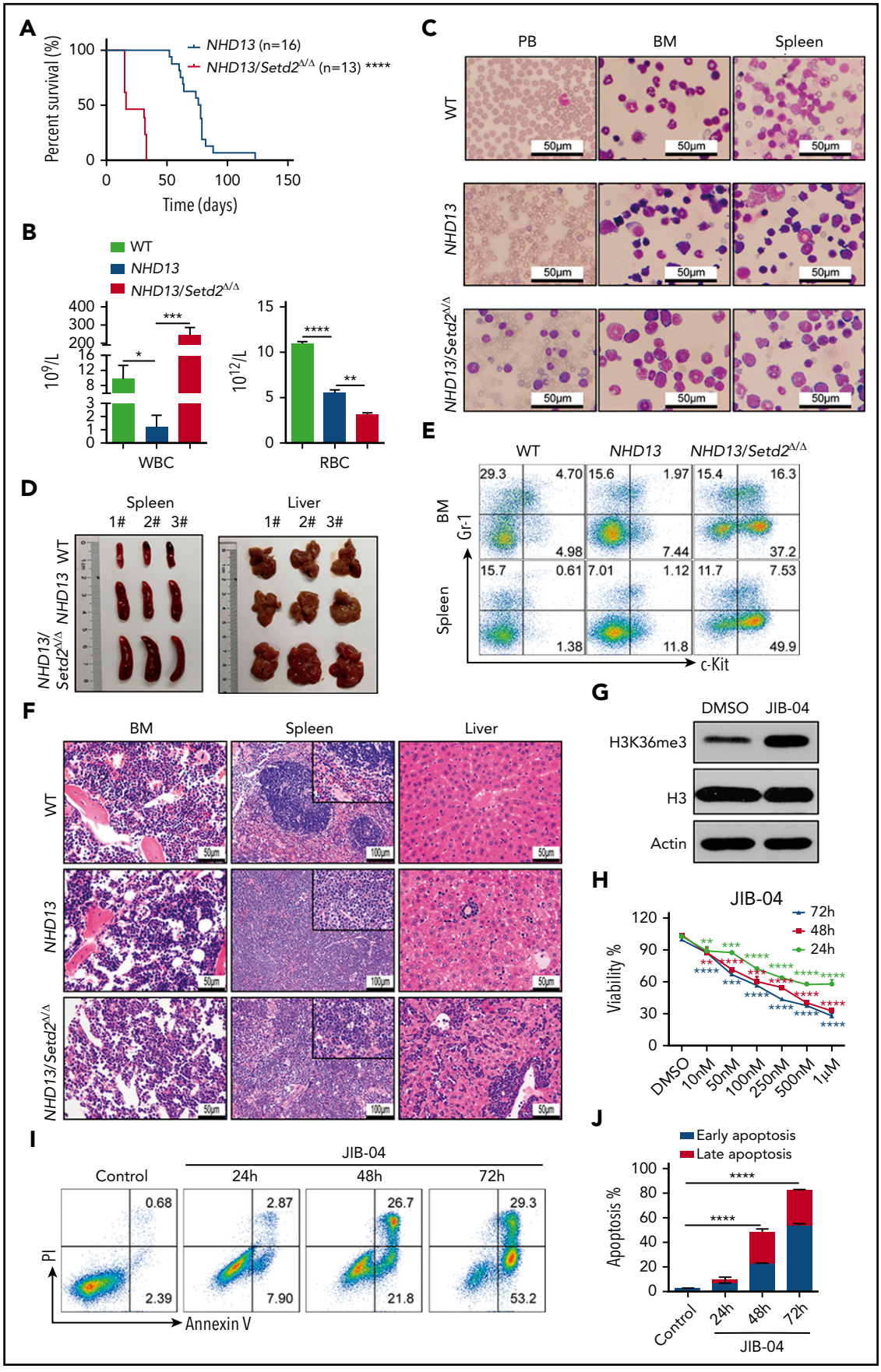

Figure 5.

Deletion of *Setd2* expands the HSPC population and enhances HSPC self-renewal in *NHD13* mice

To further understand the rapid development of leukemia observed in the *NHD13*/*Setd2*$^{\Delta/\Delta}$ mice, we analyzed the BM HSPC compartment in the mice receiving *NHD13* or *NHD13*/*Setd2*$^{\Delta/\Delta}$ BM cell transplants. We found that loss of *Setd2* did not severely impair BM cellularity (Figure 3A; supplemental Figure 5A), but rapidly altered the BM compartment of the recipient mice with a marked expansion of the Lin$^-$, Lin$^-$c-Kit$^+$Sca-1$^-$ (LK), and Lin$^-$ c-Kit$^+$Sca-1$^+$ (LSK) cells (Figure 3A-C).

To avoid the potential effect of BM ablation caused by irradiation, we analyzed the HSPCs of the primary mice at pre-MDS stage (2 months of age). The results showed that the Lin$^-$ and LK cell populations were significantly expanded in the *NHD13*/*Setd2*$^{\Delta/\Delta}$ mice compared with those in the WT and *NHD13* mice (Figure 3A; supplemental Figure 5B-C), whereas the LSK cells seemed not to be dramatically affected (supplemental Figure 5B-C). However, a more detailed analysis by separating the LSK cells into multipotential progenitors (MPPs), long-term HSCs (LT-HSCs), and short-term HSCs (ST-HSCs), based on their Flt3 and CD34 expression levels, showed that the deletion of *Setd2* increased MPPs, but not LT-HSCs or ST-HSCs, in the *NHD13* mice (Figure 3D-E). This expansion of HSPCs by *Setd2* deficiency in the *NHD13* mice was in sharp contrast to the previous observations that *Setd2* knockout in normal mice decreased HSPCs, including MPP and LSK cells,[17,18] thus suggesting differential regulation of MDS/AML and normal hematopoiesis by *Setd2*.

To investigate whether the expansion of the *NHD13*/Setd2$^{\Delta/\Delta}$ HSPCs was related to enhanced self-renewal, we used the sorted LSK cells to perform the paired daughter cell assay, which could quantify different types of symmetric and asymmetric cell divisions of individual cells by determining combinations of differentiation potentials of their daughter cells.[28] The results showed that the symmetric self-renewal division frequency of the *NHD13*/*Setd2*$^{\Delta/\Delta}$ LSK cells (38%) was much higher than that of the *NHD13* (10%) and WT (10%) LSK cells, whereas the symmetric commitment divisions were dominant in the *NHD13* LSK cells (50%) compared with the *NHD13*/*Setd2*$^{\Delta/\Delta}$ (12%) LSK cells (Figure 3F). Thus, our results suggest an important role of *Setd2* in regulating the balance between the stem cell–depleting divisions and the symmetric stem cell self-renewing divisions in the *NHD13* mouse model.

Loss of *Setd2* impairs myeloid differentiation and dysregulates the cell cycle in *NHD13* mice

We further analyzed the multipotent hematopoietic progenitors, including megakaryocyte erythroid progenitors (MEPs), granulocyte and monocyte progenitors (GMPs), and common myeloid progenitors (CMPs), in the BM of the primary mice and those receiving WT, *NHD13*, and *NHD13*/*Setd2*$^{\Delta/\Delta}$ BM cell transplants. We found that the MEPs were most dramatically increased in both the primary mice and *NHD13*/*Setd2*$^{\Delta/\Delta}$ BM-recipient mice compared with the counterpart *NHD13*-recipient mice (Figure 4A-B; supplemental Figure 5B-C). The effects of *Setd2* deletion on the frequencies and number of GMPs and CMPs were relatively marginal or variable (Figure 4A-B; supplemental Figure 5B-C). Thus, these results suggest that the loss of *Setd2* affects erythroid and megakaryocyte differentiation to a greater degree than it affects granulocyte and monocyte differentiation.

To investigate the role of *Setd2* in terminal differentiation of the *NHD13*-expressing cells, we examined erythroid differentiation in the peripheral blood (PB), BM, and spleen of the primary WT, *NHD13*, and *NHD13*/*Setd2*$^{\Delta/\Delta}$ mice. Flow cytometry analysis of cells double stained with Ter119 and CD71 was used to distinguish different erythroid developmental stages including proerythroblasts, basophilic erythroblasts, chromatophilic erythroblasts, and orthochromatophilic erythroblasts.[29,30] We observed altered erythroid differentiation stages with increased frequencies of the immature erythroid cells in the PB, BM, and spleen of the *NHD13*/*Setd2*$^{\Delta/\Delta}$ mice, compared with the WT and *NHD13* mice (Figure 4C-D). These results suggest that the deletion of *Setd2* inhibits erythroid differentiation of the *NHD13*-expressing cells, which could accelerate the progression of MDS to leukemia.

To further understand the basis of the expansion and differentiation impairment of the *NHD13*/*Setd2*$^{\Delta/\Delta}$ HSPCs, we performed a CFU assay, using HSPCs isolated from the transplant-recipient *NHD13* and *NHD13*/*Setd2*$^{\Delta/\Delta}$ mice. We found that, whereas the *NHD13* HSPCs formed very few colonies, the *NHD13*/*Setd2*$^{\Delta/\Delta}$ HSPCs showed enhanced self-renewal and gave rise to an increased number of erythroid colonies (BFU-E; Figure 4E-F). These results suggest that the improved HSPC expansion and the anemia in the *NHD13*/*Setd2*$^{\Delta/\Delta}$ mice were caused by elevated self-renewal and defects in producing erythroid progenitors. Next, we analyzed the cell cycle status of the *NHD13* and *NHD13*/*Setd2*$^{\Delta/\Delta}$ HSPCs and found that loss of *Setd2* increased the percentage of cells in the G2/M phase and reduced cell death (Figure 4G-H; supplemental Figure 5D-E). Altogether, these results suggest that loss of *Setd2* accumulates more activated HSPCs and maintains a more aggressive myeloid malignancy.

Loss of *Setd2* promotes maintenance of MDS-derived leukemia

To examine the effect of *Setd2* deficiency on the maintenance of *NHD13*-driven AML, we performed secondary BM transplantation

Figure 5. *Setd2* deficiency accelerates leukemia progression in secondary transplantation and JIB-04 regulates proliferation and apoptosis of SKM-1 cells. (A) Survival curves of the mice that underwent secondary BM transplantation from the *NHD13* (n = 16; median survival, 77 days) or *NHD13*/*Setd2*$^{\Delta/\Delta}$ (n = 13; median survival, 16 days) leukemic mice. (B) Complete blood count (CBC) analysis of *NHD13* and *NHD13*/*Setd2*$^{\Delta/\Delta}$ leukemic BM in the WT and secondary transplant-recipient mice. CBCs were obtained 16 days after transplantation. RBC, red blood cell. (C) Wright's staining of PB, BM, and spleen cells isolated from mice receiving the *NHD13* and *NHD13*/*Setd2*$^{\Delta/\Delta}$ leukemic BM for 16 days. (D) Images of the spleens and livers isolated from the mice receiving *NHD13* or *NHD13*/*Setd2*$^{\Delta/\Delta}$ leukemic BM for 16 days. (E) Representative flow cytometry profiles of Gr-1 and c-Kit expression of the BM and spleen cells of the mice receiving *NHD13* or *NHD13*/*Setd2*$^{\Delta/\Delta}$ leukemic BM for 16 days. (F) Hematoxylin and eosin staining of the BM, spleen, and liver of the mice receiving *NHD13* or *NHD13*/*Setd2*$^{\Delta/\Delta}$ leukemic BM for 16 days. (G) Western blot analysis of H3K36me3 in the JIB-04 (1 μM) or dimethyl sulfoxide–treated SKM-1 cells. (H) MTT analysis of the JIB-04 (1 μM) or dimethyl sulfoxide–treated SKM-1 cells. (I-J) Representative flow cytometry analysis (I) and quantification of the frequencies (J) of the apoptotic SKM-1 cells. *$P < .05$; **$P < .01$; ***$P < .001$; ****$P < .0001$.

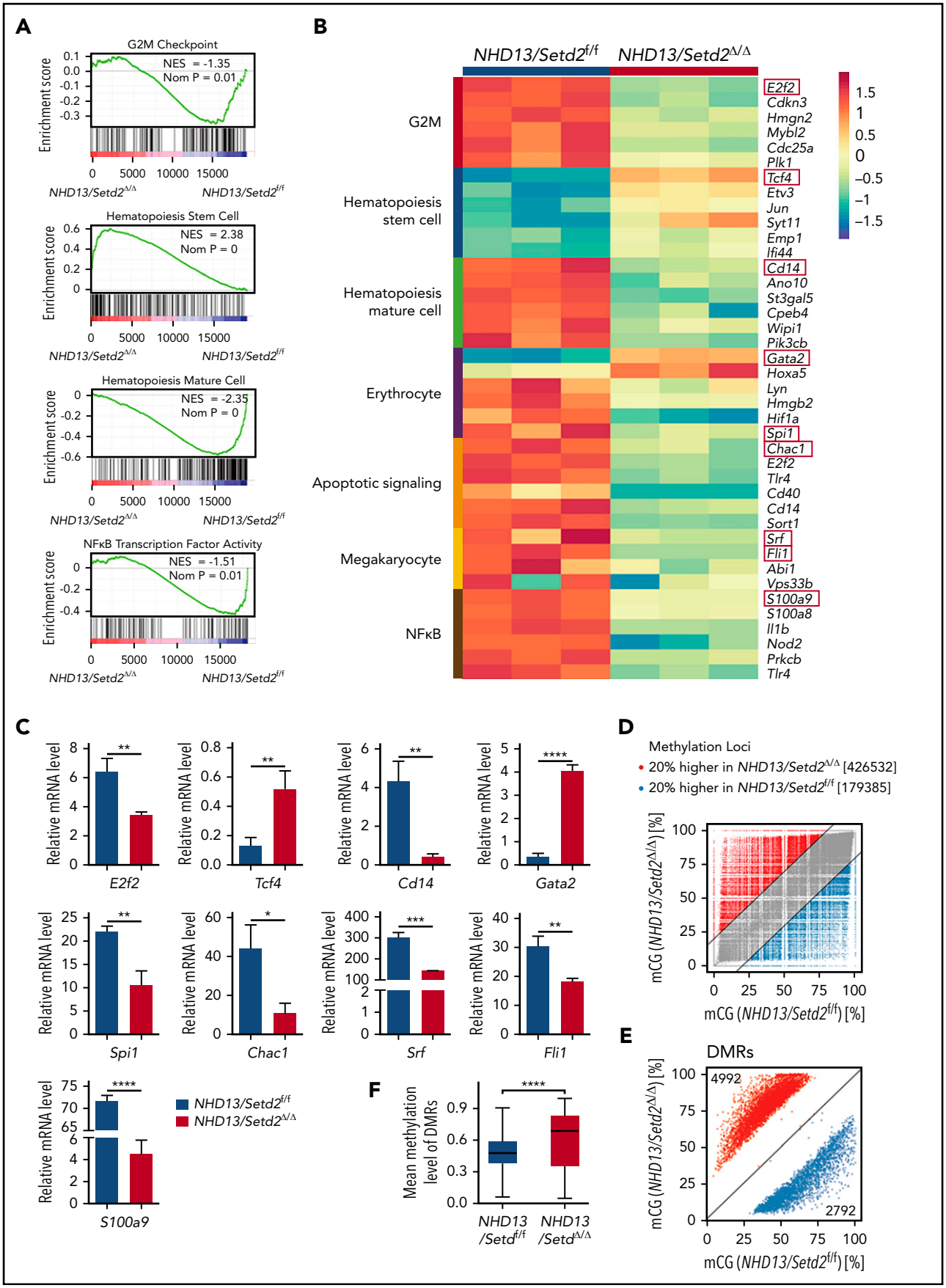

Figure 6.

by transplanting the *NHD13*-expressing WT or *Setd2*$^{\Delta/\Delta}$ BM cells collected from the primary leukemic mice into sublethally irradiated recipient mice. We found that, although these leukemias were all transplantable, the secondarily transplanted *NHD13/Setd2*$^{\Delta/\Delta}$ group had a significantly shorter survival, with higher WBC and lower red blood cell counts, compared with the *NHD13* group (Figure 5A-B). The spleens and livers of the *NHD13/Setd2*$^{\Delta/\Delta}$ leukemic mice were significantly enlarged and massively infiltrated with myeloblasts (Figure 5C-D; supplemental Figure 6A). Flow cytometry analysis showed more c-Kit^{+}Gr1^{+} and c-Kit^{+}Mac1^{+} cells in the BM and spleen compared with counts in the *NHD13* or WT mice (Figure 5E; supplemental Figure 6B-D). We also observed more leukemic blasts in the BM and spleen of the *NHD13/setd2*$^{\Delta/\Delta}$ mice (Figure 5C-F). Thus, loss of *Setd2* significantly promoted aggressiveness of *NHD13*-driven AML, which suggests that *Setd2* deficiency accelerates not only the transformation of MDS to AML, but also the progression of leukemia.

In considering that the decreased in H3K36me3 may contribute to leukemia maintenance, we tested a Jumonji histone demethylases inhibitor, JIB-04,[31] to treat the SKM-1 cell line, which was derived from human MDS-associated leukemia.[32] Western blot analysis showed that the JIB-04 treatment indeed increased H3K36me3 in the SKM-1 cells (Figure 5G). We treated the SKM-1 cells with different doses of JIB-04, and the results showed that JIB-04 significantly inhibited the growth of the SKM-1 cells in a dose-dependent manner (Figure 5H). Flow cytometry analysis showed that the JIB-04 treatment resulted in an increase in apoptosis of the SKM-1 cells (Figure 5I-J). Furthermore, we also used JIB-04 to treat the leukemia cells from the *NHD13* and *NHD13/Setd2*$^{\Delta/\Delta}$ mice, and the results showed that *NHD13/Setd2*$^{\Delta/\Delta}$ cells were less sensitive to JIB-04 treatment than were the *NHD13* cells (supplemental Figure 6E-F), probably because of the inability of the *NHD13/Setd2*$^{\Delta/\Delta}$ cells to increase H3K36me3. These results suggest that increasing H3K36me3 may be a strategy or an effective indicator in the treatment of MDS-associated leukemia.

RNA-seq and whole-genome bisulfate sequencing analysis reveal a unique gene signature in *Setd2*-deleted *NHD13* HSPCs

To understand how *Setd2* deficiency promotes the transformation from MDS to leukemia, we performed comparative RNA-seq analysis of HSPCs from the *NHD13* and *NHD13/setd2*$^{\Delta/\Delta}$ primary mice. Notably, a comparison with the previously reported data of *Setd2* knockout in WT HSPCs[17] showed that the majority (97.6%) of altered genes by *Setd2* deletion in the NHD13 HSPCs were different from those in the WT, suggesting a context dependency of the Setd2 target genes (supplemental Figure 7A-B). Gene Set Enrichment Analysis revealed that at the G2/M checkpoint, NF-κB and hematopoiesis mature gene sets were depleted of *NHD13/Setd2*$^{\Delta/\Delta}$ HSPCs, whereas the HSC gene sets were enriched (Figure 6A), consistent with the phenotypic differences between the AML and MDS stages. Some genes that were dysregulated in the *NHD13/Setd2*$^{\Delta/\Delta}$ HSPCs (eg, *S100a9*, *E2f2*, *Tcf4*, *Cd14*, *Chac1*, *Spi1*, *Gata2*, *Fli1*, and *Srf*) have been shown to play important roles in regulating these pathways (Figure 6B). The altered expression of these genes was validated by qPCR (Figure 6C). Thus, these results further support and provide possible mechanistic explanations for the enhanced self-renewal, impaired differentiation, and cell cycle abnormalities of *NHD13/Setd2*$^{\Delta/\Delta}$ HSPCs.

It has been reported that H3K36me3 can be recognized by Dnmt3a/b, suggesting that Setd2 could be functionally connected with Dnmt3a/b-mediated DNA methylation.[33-35] Thus, we examined the change in DNA methylation by *Setd2* deletion in the *NHD13* mice. We performed whole-genome bisulfate sequencing (WGBS) analysis of the *NHD13* and *NHD13/Setd2*$^{\Delta/\Delta}$ LSK cells, and we found that the *NHD13/Setd2*$^{\Delta/\Delta}$ cells had more hypermethylated loci than the *NHD13* cells (2.4-fold; Figure 6D) and that their differentially methylated regions (DMRs) were also more enriched in the hypermethylated loci (1.8-fold; Figure 6E; supplemental Figure 7C). The mean methylation level of the DMRs was also significantly higher in the *NHD13/Setd2*$^{\Delta/\Delta}$ than the *NHD13* cells (Figure 6F). Moreover, the DNA methylation profiling showed that the *NHD13/Setd2*$^{\Delta/\Delta}$ genome had decreased CpG methylation levels in the gene body regions but increased levels in the intergenic regions (supplemental Figure 7D-F), which may explain its overall hypermethylation state. Pathway analysis of the MDR-associated genes showed considerable overlaps with the gene expression profiles (supplemental Figure 7G-H). These results demonstrate the altered DNA methylation pattern that may be important for Setd2-regulated gene expression and the *NHD13*-expressing HSPC functions.

S100a9, a target gene of *Setd2*, rescues the phenotype of *Setd2* deficiency in *NHD13* HSPCs

To identify functionally important *Setd2* target genes and to understand the regulatory mechanism, we performed ChIP-seq analysis of the c-Kit^{+} cells of the *NHD13* and *NHD13/Setd2*$^{\Delta/\Delta}$ mice with an anti-H3K36me3 antibody. A significant decrease in H3K36me3 on the gene body regions of active genes was detected in the *NHD13/Setd2*$^{\Delta/\Delta}$ cells compared with levels in the *NHD13* controls (Figure 7A; supplemental Figure 8A-C). Given the important role of the cross talk between H3K36me3 and DNA methylation in leukemogenesis, we also surveyed the dysregulated genes that associate with the DMRs. We found that *S100a9*, which encodes a calcium-binding protein, was significantly downregulated by *Setd2* deletion in the *NHD13* mice (Figure 6B-C; supplemental Figure 8D-E), accompanied by a decreased H3K36me3 level (Figure 7B). Meanwhile, *S100a9* fell into the category of genes with DMR-associated expression

Figure 6. Gene expression profiling and whole genome methylation analysis of the *Setd2*-deleted *NHD13* HSPCs. (A) RNA-seq and Gene Set Enrichment Analysis of the BM HSPCs of the WT, *NHD13/Setd2*$^{f/f}$, and *NHD13/Setd2*$^{\Delta/\Delta}$ mice at 4 weeks after poly(I:C) injection. (B) Gene expression profiles revealing the differentially expressed genes in the pathways regulating the G2M checkpoint, HSC maintenance and differentiation, erythrocytes, megakaryocytes, apoptosis, and NF-κB targets. (C) qPCR analysis of representative genes of interest, which are labeled with red boxes in panel B. (D) Comparison of relative methylation differences between the BM HSPCs of the *NHD13/Setd2*$^{f/f}$ and *NHD13/Setd2*$^{\Delta/\Delta}$ mice at 4 weeks after poly(I:C) injection. Each dot represents a methylation locus that was detected >10 times. (E) Number of hypomethylated (2792) and hypermethylated (4992) DMRs. Each dot represents a DMR. (F) Comparison of average methylation levels of all DMRs between the *NHD13/Setd2*$^{f/f}$ and *NHD13/Setd2*$^{\Delta/\Delta}$ BM HSPCs. *$P < .05$; **$P < .01$; ***$P < .001$; ****$P < .0001$.

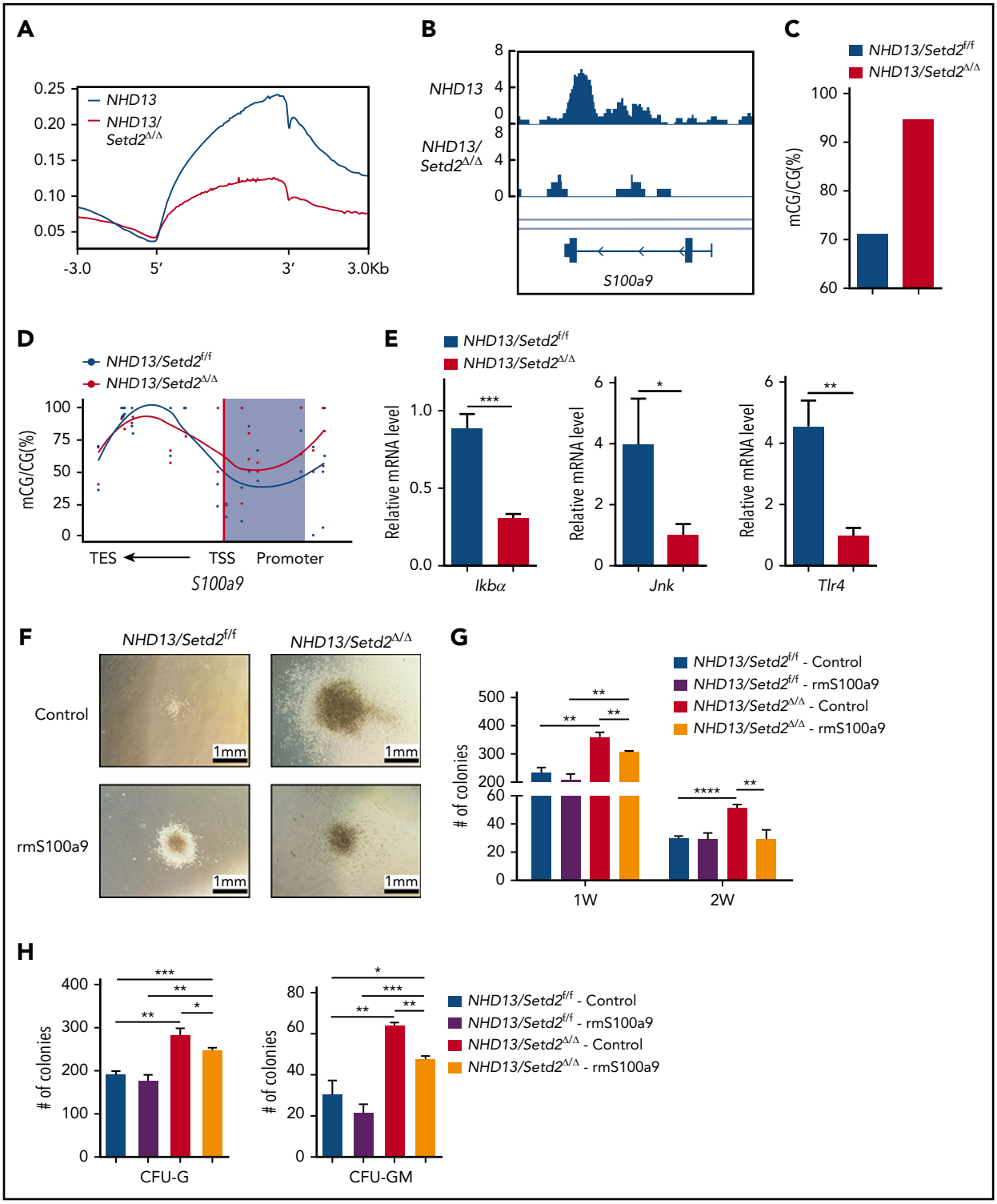

Figure 7. *S100a9* is directly regulated by Setd2, and restoration of S100a9 abrogates the effect of *Setd2* deficiency on the *NHD13* HSPCs. (A) A profile of H3K36me3 across the gene body and the upstream (5′) and downstream (3′) regions. ChIP-seq analyses were performed with spleen c-Kit$^+$ cells isolated from the *NHD13* and *NHD13/Setd2*$^{\Delta/\Delta}$ mice at leukemia stage. (B) A decrease occurred in H3K36me3 in the *S100a9* gene locus of the *NHD13/Setd2*$^{\Delta/\Delta}$ cells relative to that in the *NHD13* cells. (C-D) Different DNA methylation in the *S100a9* promoter (C) and a profile of DNA methylation across the *S100a9* gene locus (D) in the *NHD13* and *NHD13/Setd2*$^{\Delta/\Delta}$ cells. TSS, transcription start sites; TES, transcription end sites; the shading denotes the promoter region. (E) qPCR analysis of *Ikba*, *Jnk*, and *Tlr4* in the *NHD13* and *NHD13/Setd2*$^{\Delta/\Delta}$ cells. (F) Micrographs of representative colonies in the CFU assays with the *NHD13* and *NHD13/Setd2*$^{\Delta/\Delta}$ HSPCs. Cells (3×10^3) were plated for each assay. Recombinant mouse S100a9 protein (rmS100a9) was added at a final concentration of 4 μg/mL. (G-H) The number of indicated colonies in the CFU assays. CFU-G and CFU-GM were counted 1 week after plating. $^*P < .05$; $^{**}P < .01$; $^{***}P < .001$; $^{****}P < .0001$.

(Figure 7C-D). qPCR analysis of human MDS BM samples also showed a relatively lower expression of *S100A9* compared with samples from healthy subjects (supplemental Figure 8F). Overexpression of *SETD2* in SKM-1 cells upregulated *S100A9* and *S100A8* (supplemental Figure 8G) and decreased colony formation by the cells (supplemental Figure 8H-I). Thus, we identified *S100a9* as a target gene of *Setd2* based on RNA-seq, ChIP-seq, and whole-genome bisulfate sequencing (WGBS) analyses.

S100a9 has been reported to trigger cell death of HSPCs, including MEPs, and to contribute to ineffective hematopoiesis in MDS.[36-38] S100A9 has also been identified as a differentiation inducer in AML.[39] Mechanistically, it has been shown that the activation of the JNK and NF-κB signaling pathways is essential in S100A9-induced AML differentiation through Toll-like receptor 4 in leukemia cells.[39] We indeed found that the expression of *Tlr4* and the Jnk/NF-κB pathway–related genes, such as *Jnk* and *Ikba*, was decreased in the *NHD13*/*Setd2*$^{\Delta/\Delta}$ HSPCs (Figure 7E), which is consistent with the Kyoto Encyclopedia of Genes and Genome analysis showing the MAPK signaling pathway to be significantly regulated by *Setd2* in *NHD13* HSPCs (supplemental Figure 7G). To understand the role of *S100a9* in *NHD13*/*Setd2*$^{\Delta/\Delta}$ HSPCs, we performed a CFU assay using sorted HSPCs that were treated with 4 μg/mL recombinant mouse S100a9 protein (rmS100a9). We found that the rmS100a9 treatment reduced the promoted expansion of the *NHD13*/*Setd2*$^{\Delta/\Delta}$ HSPCs, including the capacity of generating various types of colonies (Figure 7F-H). Conversely, knockdown of *S100a9* accelerated the progression of AML in the *NHD13* mice (supplemental Figure 8G-I). Last, S100A9 could be upregulated in SKM-1 cells by treatment with JIB-04, especially when SETD2 was suppressed by shRNA-mediated knockdown (supplemental Figure 8M-N). Thus, the mimicking and rescue of the phenotypes of *Setd2* deficiency in the MDS-associated HSPCs by manipulation of S100a9 suggests that *S100a9* downregulation contributes to the increased self-renewal and defective myeloid differentiation in the *NHD13*/*Setd2*$^{\Delta/\Delta}$ mice.

Discussion

In this study, low expression of *SETD2* predicted a poor outcome in MDS and identified a previously unrecognized function of Setd2 in an *NHD13*-driven MDS mouse model: controlling the progression of MDS to leukemia. Deletion of *Setd2* significantly accelerated development of AML, indicating that Setd2 acts as an important tumor suppressor in the transformation of *NHD13*-driven MDS to AML. Mechanistically, loss of *Setd2* enhanced self-renewal and impaired myeloid differentiation in the *NHD13*-expressing HSPCs. Early progression of MDS to AML in *Setd2*-deleted *NHD13* mice was also associated with abnormal erythroid differentiation and reduced cell death. Symmetric self-renewal division was increased by *Setd2* deletion in the *NHD13*-expressing HSCs, which may also account for the higher risk for the development of leukemia in the *NHD13*/*Setd2*$^{\Delta/\Delta}$ mice.[40] The *NHD13*/*Setd2*$^{\Delta/\Delta}$ mice developed less differentiated AML, which may reflect differentiation blocking in the early stage and enhanced self-renewal of leukemia-initiating cells, induced by *Setd2* deletion.

When MDS progressed to AML, there was increased cell survival and decreased cell death. Loss of *Setd2* triggered a unique gene signature in the *NHD13*-expressing HSPCs at both the MDS and AML stages, including upregulation of the HSC pathway and downregulation of the myeloid cell differentiation pathway. It appears that elevated MAPK signaling induced by *Setd2* deletion in the *NHD13* BM cells confers a growth advantage to the preleukemic blasts. We identified *S100a9* as a target gene of *Setd2* in the *NHD13* leukemic cells. S100A9 and S100A8 have been implicated in the pathology of *RPS14*-associated MDS and regulation of myeloid and erythroid differentiation,[39,41] and, in particular, S100A9 can induce AML differentiation, whereas S100A8 inhibits differentiation induced by S100A9.[39] In the *NHD13* MDS model, S100a9 acts to prevent the transformation to AML. Although S100a9 and S100a8 are highly homologous, these 2 proteins may have opposite functions in *NHD13*-mediated leukemogenesis.

We observed different effects of *Setd2* deletion in the HSPCs of MDS/AML relative to that of normal hematopoiesis. *Setd2* exerts cellular context–specific effects in HSPCs, as the decrease in LSK and MPP cells was found in the *Setd2*$^{\Delta/\Delta}$ mice, but not in the *NHD13*/*Setd2*$^{\Delta/\Delta}$ mice. The *NHD13*/*Setd2*$^{\Delta/\Delta}$ mice had an increased WBC count and decreased HGB, but the *Setd2*$^{\Delta/\Delta}$ mice had a decreased WBC count and normal HGB. Intriguingly, the Setd2-regulated genes including *S100a9* are significantly different in the *NHD13* and WT cells, which may cause the genetic background–specific effects of *Setd2*. Thus, our experiments showed that *Setd2* deletion–induced transformation differs in WT and *NHD13* HSPCs.

Altogether, our results suggest that deficiency in *Setd2* function promotes the progression of MDS to AML. Moreover, the low expression of *SETD2* correlates strongly with the survival of patients with MDS. Our findings indicate that promoting *SETD2* function or activating downstream effects of *SETD2* may be helpful in elimination of MDS-associated leukemia.

Acknowledgments

The authors thank Dangsheng Li for critical reading and helpful comments on the manuscript and Y. Zhai, X. Miao, S. Yan, Y. Chen, K. Wang, and Y. Wang (Shanghai Institute of Nutrition and Health core facilities) for technical support.

This work was supported by National Key Research and Development Plan of China grants 2018YFA0107200, 2018YFA0800203 (L.W.), and 2018YFA0107802 (X.-J.S.); National Natural Science Foundation of China (NSFC) General Program grants 81670122, 81970150 (L.W.), and 81670094 (X.-J.S.); NSFC Excellent Young Scholar Program grant 81622003 (L.W.); CAS Bureau of Major R&D Program grant XDA12020376 (L.W.); the CAS Bureau of Frontier Sciences and Education Program grant QYZDBSSWSMC027 (L.W.); Shanghai Municipal Education Commission-Gaofeng Clinical Medicine grant 20152506 (X.-J.S.); Shanghai Collaborative Innovation Program on Regenerative Medicine and Stem Cell Research 2019CXJQ01 (S.-J.C., X.-J.S.); Innovative Research Team of High-Level Local Universities in Shanghai (X.-J.S.); Shanghai Guangci Translational Medical Research Development Foundation; and the Samuel Waxman Cancer Research Foundation.

Authorship

Contribution: L.W., X.-J.S., and B.-Y.C. designed the research, analyzed the data, and wrote the paper; B.-Y.C., J.S., C.-L.H., S.-B.C., Q.Z.,

J.-C.W., D.H., M.S., N.L., P.-C.Y., P.L., J.-Y.Z., and R.-F.D. performed the research; and S.-J.C., Z.C., S.D.N., Q.Z., C.-H.X. Y.-L.Z., S.-J.Z., F.L., L.-J.Z., and Q.-H.H. analyzed the data and contributed new tools.

Conflict-of-interest disclosure: The authors declare no competing financial interests.

ORCID profiles: S.-B.C., 0000-0001-7298-2451; C.-H.X., 0000-0002-3836-3179; J.-C.W., 0000-0002-8211-2801; P.-C.Y., 0000-0002-7256-2489; J.-Y.Z., 0000-0001-7820-5039; X.-J.S., 0000-0001-8826-4614.

Correspondence: Lan Wang, Shanghai Institute of Nutrition and Health, Shanghai Institutes for Biological Sciences, Chinese Academy of Sciences, Shanghai 200031, China; e-mail: lwang@sibs.ac.cn; and Xiao-Jian Sun, Shanghai Institute of Hematology, Ruijin Hospital, Shanghai Jiao Tong University School of Medicine, Shanghai 200025, China; e-mail: xjsun@sibs.ac.cn.

Footnotes

Submitted 28 August 2019; accepted 8 March 2020; prepublished online on *Blood* First Edition 20 March 2020. DOI 10.1182/blood.2019001963.

*B.-Y.C., J.S., and C.-L.H. are joint first authors.

The RNA-seq, ChIP-seq, and WGBS data reported in this article were deposited in the Gene Expression Omnibus database (accession number GSE129691).

The online version of this article contains a data supplement.

The publication costs of this article were defrayed in part by page charge payment. Therefore, and solely to indicate this fact, this article is hereby marked "advertisement" in accordance with 18 USC section 1734.

REFERENCES

1. Sperling AS, Gibson CJ, Ebert BL. The genetics of myelodysplastic syndrome: from clonal haematopoiesis to secondary leukaemia. *Nat Rev Cancer*. 2017;17(1):5-19.
2. Corey SJ, Minden MD, Barber DL, Kantarjian H, Wang JC, Schimmer AD. Myelodysplastic syndromes: the complexity of stem-cell diseases. *Nat Rev Cancer*. 2007;7(2):118-129.
3. Lin YW, Slape C, Zhang Z, Aplan PD. NUP98-HOXD13 transgenic mice develop a highly penetrant, severe myelodysplastic syndrome that progresses to acute leukemia. *Blood*. 2005;106(1):287-295.
4. Xu H, Menendez S, Schlegelberger B, et al. Loss of p53 accelerates the complications of myelodysplastic syndrome in a NUP98-HOXD13-driven mouse model. *Blood*. 2012;120(15):3089-3097.
5. Abdel-Wahab O, Adli M, LaFave LM, et al. ASXL1 mutations promote myeloid transformation through loss of PRC2-mediated gene repression. *Cancer Cell*. 2012;22(2):180-193.
6. Haferlach T, Nagata Y, Grossmann V, et al. Landscape of genetic lesions in 944 patients with myelodysplastic syndromes. *Leukemia*. 2014;28(2):241-247.
7. Sashida G, Harada H, Matsui H, et al. Ezh2 loss promotes development of myelodysplastic syndrome but attenuates its predisposition to leukaemic transformation. *Nat Commun*. 2014;5(1):4177.
8. Xu L, Gu ZH, Li Y, et al. Genomic landscape of CD34+ hematopoietic cells in myelodysplastic syndrome and gene mutation profiles as prognostic markers. *Proc Natl Acad Sci USA*. 2014;111(23):8589-8594.
9. Cao Q, Gearhart MD, Gery S, et al. BCOR regulates myeloid cell proliferation and differentiation. *Leukemia*. 2016;30(5):1155-1165.
10. Maegawa S, Gough SM, Watanabe-Okochi N, et al. Age-related epigenetic drift in the pathogenesis of MDS and AML. *Genome Res*. 2014;24(4):580-591.
11. Bejar R, Stevenson K, Abdel-Wahab O, et al. Clinical effect of point mutations in myelodysplastic syndromes. *N Engl J Med*. 2011;364(26):2496-2506.
12. Cheng G, Liu F, Asai T, et al. Loss of p300 accelerates MDS-associated leukemogenesis. *Leukemia*. 2017;31(6):1382-1390.
13. Santini V. How I treat MDS after hypomethylating agent failure. *Blood*. 2019;133(6):521-529.
14. Sun XJ, Wei J, Wu XY, et al. Identification and characterization of a novel human histone H3 lysine 36-specific methyltransferase. *J Biol Chem*. 2005;280(42):35261-35271.
15. Hu M, Sun XJ, Zhang YL, et al. Histone H3 lysine 36 methyltransferase Hypb/Setd2 is required for embryonic vascular remodeling. *Proc Natl Acad Sci USA*. 2010;107(7):2956-2961.
16. Licht JD. SETD2: a complex role in blood malignancy. *Blood*. 2017;130(24):2576-2578.
17. Zhang YL, Sun JW, Xie YY, et al. Setd2 deficiency impairs hematopoietic stem cell self-renewal and causes malignant transformation. *Cell Res*. 2018;28(4):476-490.
18. Zhou Y, Yan X, Feng X, et al. *Setd2* regulates quiescence and differentiation of adult hematopoietic stem cells by restricting RNA polymerase II elongation. *Haematologica*. 2018;103(7):1110-1123.
19. Patnaik MM, Abdel-Wahab O. SETD2: linking stem cell survival and transformation. *Cell Res*. 2018;28(4):393-394.
20. Zhu X, He F, Zeng H, et al. Identification of functional cooperative mutations of SETD2 in human acute leukemia. *Nat Genet*. 2014;46(3):287-293.
21. Mar BG, Bullinger LB, McLean KM, et al. Mutations in epigenetic regulators including SETD2 are gained during relapse in paediatric acute lymphoblastic leukaemia. *Nat Commun*. 2014;5(1):3469.
22. Wang S, Yuan X, Liu Y, et al. Genetic polymorphisms of histone methyltransferase SETD2 predicts prognosis and chemotherapy response in Chinese acute myeloid leukemia patients. *J Transl Med*. 2019;17(1):101.
23. Mar BG, Chu SH, Kahn JD, et al. *SETD2* alterations impair DNA damage recognition and lead to resistance to chemotherapy in leukemia. *Blood*. 2017;130(24):2631-2641.
24. Dong Y, Zhao X, Feng X, et al. SETD2 mutations confer chemoresistance in acute myeloid leukemia partly through altered cell cycle checkpoints. *Leukemia*. 2019;33(11):2585-2598.
25. Skucha A, Ebner J, Schmöllerl J, et al. MLL-fusion-driven leukemia requires SETD2 to safeguard genomic integrity. *Nat Commun*. 2018;9(1):1983.
26. Watatani Y, Nagata Y, Grossmann V, et al. Two Novel Distinct Subtypes of Myeloid Neoplasms Molecularly Associated with Histone H3K36 Methylations [abstract]. *Blood*. 2015;126(23). Abstract 2841.
27. Pellagatti A, Cazzola M, Giagounidis A, et al. Deregulated gene expression pathways in myelodysplastic syndrome hematopoietic stem cells. *Leukemia*. 2010;24(4):756-764.
28. Takano H, Ema H, Sudo K, Nakauchi H. Asymmetric division and lineage commitment at the level of hematopoietic stem cells: inference from differentiation in daughter cell and granddaughter cell pairs. *J Exp Med*. 2004;199(3):295-302.
29. Socolovsky M, Nam H, Fleming MD, Haase VH, Brugnara C, Lodish HF. Ineffective erythropoiesis in Stat5a(-/-)5b(-/-) mice due to decreased survival of early erythroblasts. *Blood*. 2001;98(12):3261-3273.
30. Mortensen M, Ferguson DJ, Edelmann M, et al. Loss of autophagy in erythroid cells leads to defective removal of mitochondria and severe anemia in vivo. *Proc Natl Acad Sci USA*. 2010;107(2):832-837.
31. Wang L, Chang J, Varghese D, et al. A small molecule modulates Jumonji histone demethylase activity and selectively inhibits cancer growth [published correction appears in *Nat Commun*. 2013;4:2639]. *Nat Commun*. 2013;4(1):2035.
32. Nakagawa T, Matozaki S, Murayama T, et al. Establishment of a leukaemic cell line from a patient with acquisition of chromosomal abnormalities during disease progression in myelodysplastic syndrome. *Br J Haematol*. 1993;85(3):469-476.
33. Dhayalan A, Rajavelu A, Rathert P, et al. The Dnmt3a PWWP domain reads histone 3 lysine 36 trimethylation and guides DNA methylation. *J Biol Chem*. 2010;285(34):26114-26120.

34. Baubec T, Colombo DF, Wirbelauer C, et al. Genomic profiling of DNA methyltransferases reveals a role for DNMT3B in genic methylation. *Nature*. 2015;520(7546):243-247.

35. Neri F, Rapelli S, Krepelova A, et al. Intragenic DNA methylation prevents spurious transcription initiation. *Nature*. 2017;543(7643):72-77.

36. Chen X, Eksioglu EA, Zhou J, et al. Induction of myelodysplasia by myeloid-derived suppressor cells. *J Clin Invest*. 2013;123(11):4595-4611.

37. Basiorka AA, McGraw KL, Eksioglu EA, et al. The NLRP3 inflammasome functions as a driver of the myelodysplastic syndrome phenotype. *Blood*. 2016;128(25):2960-2975.

38. Cheng P, Eksioglu EA, Chen X, et al. S100A9-induced overexpression of PD-1/PD-L1 contributes to ineffective hematopoiesis in myelodysplastic syndromes. *Leukemia*. 2019;33(8):2034-2046.

39. Laouedj M, Tardif MR, Gil L, et al. S100A9 induces differentiation of acute myeloid leukemia cells through TLR4. *Blood*. 2017;129(14):1980-1990.

40. Wu M, Kwon HY, Rattis F, et al. Imaging hematopoietic precursor division in real time. *Cell Stem Cell*. 2007;1(5):541-554.

41. Schneider RK, Schenone M, Ferreira MV, et al. Rps14 haploinsufficiency causes a block in erythroid differentiation mediated by S100A8 and S100A9. *Nat Med*. 2016;22(3):288-297.